DELPHI Collaboration

DELPHI 2001-058 CONF 486
10 June, 2001

Measurement of Helicity Components of the Fragmentation Function

O. Smirnova, Ch. Zacharatou Jarlskog, T. Sjöstrand
Lund University

Abstract

A study of the helicity components of the fragmentation function in Z^0 hadronic decays, including estimations of hadronization corrections, has been performed. The hadronization corrections were done using clustering to reconstruct parton directions. A range of clustering cut-off values has been considered. The corrected longitudinal component of the fragmentation function was used to extract the strong coupling constant. For the preferred clustering cut-off value, we have obtained

$$\alpha_s = 0.1083 \pm 0.0012(\text{stat}) \pm 0.0119(\text{syst})$$

Contributed Paper for EPS HEP 2001 (Budapest) and LP01 (Rome)

1 Introduction

Transverse and longitudinal helicity components of the fragmentation function in hadronic decays of Z^0 have been used by the LEP experiments to extract the gluon fragmentation function, and to measure the strong coupling constant, along with other observables [1, 2, 3]. The inclusive nature of measurements implies high accuracy, thus being particularly appealing for precision studies. However, in this case, the issue of higher-order and non-perturbative corrections becomes important.

The double-differential cross-section for the hadroproduction process, $e^+e^- \to h + X$, where a hadron, h, has been measured in the final state, can be written as [4]

$$\frac{d^2\sigma^h}{dx_p\, d\cos\theta} = \frac{3}{8}(1+\cos^2\theta)\frac{d\sigma_T^h}{dx_p} + \frac{3}{4}\sin^2\theta\frac{d\sigma_L^h}{dx_p} + \frac{3}{4}\cos\theta\frac{d\sigma_A^h}{dx_p} \; , \qquad (1)$$

where subscripts T and L denote the contributions from transverse and longitudinal polarisation states of the Z^0 with respect to the $q\overline{q}$ axis, respectively, θ is the polar angle of the hadron with respect to the beam axis, and subscript A denotes the forward-backward asymmetry term.

Transverse and longitudinal components of the fragmentation function receive their major contributions from the fragmentation of quarks and gluons, respectively. The asymmetry component is equal to zero in inclusive measurements, when no distinction between particles and antiparticles is made, and will not be considered further.

This paper presents the extraction of the helicity components of the fragmentation function from data taken by the DELPHI detector in 1992-1995 at Q=91.2 GeV and is meant as an update to the previous DELPHI analysis presented in ref. [1]. It includes the new method for taking into account hadronization corrections, demonstrating the effect of latter on the measured fragmentation function values and the strong coupling constant.

2 The measured distributions

The data were collected by the DELPHI detector at the Z^0 peak, in the 1992-1995 running periods. Only charged particles were taken into account, if they satisfied following selection criteria (compare with [1]):

- impact parameter with respect to the beam crossing point below 5 cm in the transverse plane and below 10 cm along the beam axis,
- measured track length above 50 cm,
- momentum between 0.1 GeV/c and 50 GeV/c,
- polar angle between 11° and 169°,
- momentum measurement error, $\Delta p/p$, less than 100%.

An event was selected if it had:

- at least 5 tracks with $p > 0.2$ GeV/c;
- total energy above 15 GeV (assuming the $\pi^\pm$ mass for the particles);
- energy of the forward and backward hemispheres (with respect to the sphericity axis) above 3 GeV;

– sphericity axis polar angle between 26° and 154°;
– momentum imbalance below 20 GeV/c.

There were about 2.1 million hadronic events selected by applying the above cuts.

For each particle, its relative momentum, x_p, and polar angle cosine $\cos\theta$, was measured, and histogrammed in a two-dimensional distribution, corresponding to the double-differential cross section of 1. The range of the fractional momentum, x_p, of the particle was divided into 22 non-equidistant bins with smaller bins at low values (the momentum intervals are given, e.g., in Table 1). The range of the cosine of the polar angle of the track, $\cos\theta$, was split into 40 equidistant bins.

2.1 Correction factors

The raw data were corrected for the acceptance and resolution of the detector, detector inefficiencies, kinematic cuts, initial state radiation and secondary interactions with the detector's material. The correction factors were calculated with events initially generated with the DELPHI-tuned [5] JETSET 7.3 generator [6] and then processed by the detector simulation (simulated events, for an ideal detector) and the data reconstruction program (reconstructed events). The track and event selection cuts for the reconstructed events were the same as for the real data. The correction factors of a given interval i in x_p and $\cos\theta$ were obtained by dividing the simulated by the reconstructed distribution in this interval:

$$C_i(x_p, \cos\theta) = \frac{f_i(x_p, \cos\theta)_{simulated}}{f_i(x_p, \cos\theta)_{reconstructed}} \tag{2}$$

The corrections factors were extracted according to Eq.(2) for each of the x_p and $\cos\theta$ bins separately. There were about 11 million simulated events and 8 million reconstructed Monte Carlo events used in the analysis. The corrected double differential cross sections were then given by

$$\sigma_i^{corr} = \frac{1}{\sigma_{tot}} \frac{d^2\sigma_i}{dx_p d\cos\theta} = C_i(x_p, \cos\theta) D_i^{meas} \tag{3}$$

where D_i^{meas} are the measured distributions and C_i are the correction factors (Eq.(2)). The index refers to x_p and $\cos\theta$ bins.

3 Fragmentation function extraction

The transverse and longitudinal components of the fragmentation function are defined by normalising the corresponding differential cross sections to the total cross section, $\sigma_{tot} = \sigma_T + \sigma_L$:

$$F_T(x_p) = \frac{1}{\sigma_{tot}} \frac{d\sigma_T}{dx_p} \quad , \qquad F_L(x_p) = \frac{1}{\sigma_{tot}} \frac{d\sigma_L}{dx_p} \ . \tag{4}$$

The fragmentation functions $F_T(x_p)$ and $F_L(x_p)$ of Eq.(4), were extracted with the weighting method [4]:

$$F_P(x_p) = \int_{-v}^{+v} W_P(\cos\theta, v) \left[\frac{d^2\sigma}{dx_p \, d\cos\theta} \right] d\cos\theta \ , \tag{5}$$

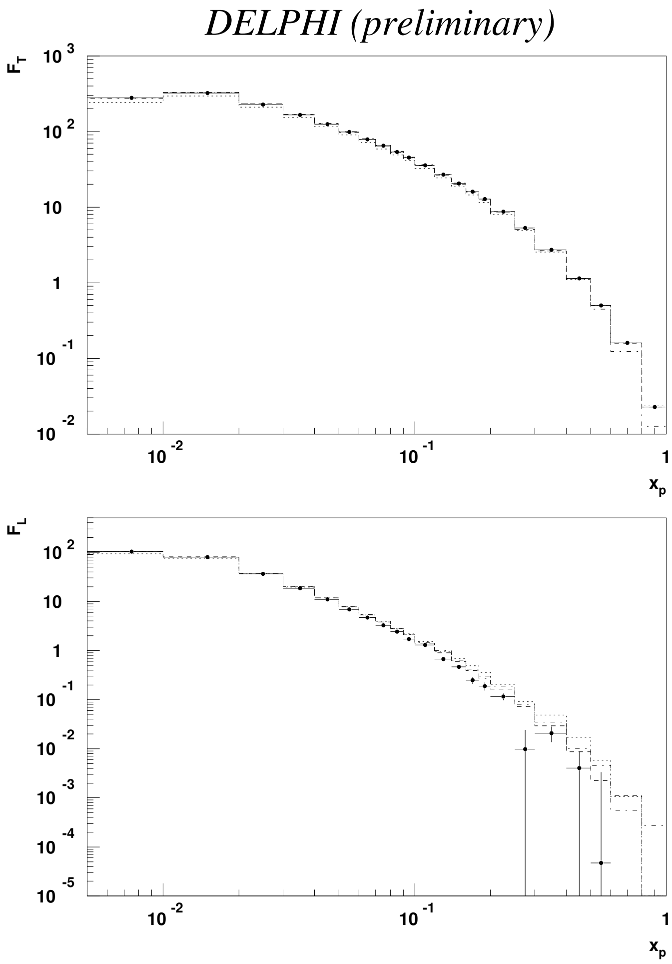

Figure 1: The transverse and longitudinal components of the fragmentation function, F_T and F_L, calculated from weights (Eq.(5)). The points (solid line) are the data, the dashed line is the DELPHI simulation, the dotted line is the DELPHI-tuned generator JETSET 7.3 and the dashed-dotted line is JETSET 7.4 with default (non-tuned) parameters.

where $P = T, L$, $v = |\cos\theta|_{max}$ is the angular range limit (usually defined by the experimental acceptance), and W_P are the weighting functions:

$$\begin{aligned} W_T(\cos\theta, v) &= [5\cos^2\theta(3 - v^2) - v^2(5 - 3v^2)]/2v^5 \ , \\ W_L(\cos\theta, v) &= [v^2(5 + 3v^2) - 5\cos^2\theta(3 + v^2)]/4v^5 \ . \end{aligned} \tag{6}$$

For the extraction of the transverse (denoted by the subscript T) and longitudinal (L) components, nine equidistant values of v were considered, between 0.95 and 0.55. It was found that the measurement becomes stable at $v = 0.85$, which was chosen as the working interval. The fragmentation functions thus obtained are shown in Figure 1 and in first columns of Tables 1 and 2. The first error quoted is the statistical one, and the second is systematics (see Section 3.1).

In Figure 1, the comparison between the data and the three curves of simulated events shows that F_L from data is systematically below all simulations in almost all of the momentum interval, whereas this is not seen that much in F_T. This might be due to the fact that F_L is more sensitive than F_T to the specifics of the fragmentation process. Also note that the full matrix-element angular orientation expressions are not included in the JETSET shower. Moreover, the comparison shows that the tuned generation is below the DELPHI simulation curve. A disagreement was expected due to the properties of the simulated events. JETSET 7.4 seems to describe the data better than the tuned generation. It was not used by the collaboration for the production of the Monte Carlo samples, as it was not available when the tuned version was produced.

3.1 Systematic uncertainties

The systematic errors were estimated by varying the criteria for the track and event selection and by modifying the extraction methods for the sample of the nominal selection (Section 2).

In order to estimate errors due to the selection criteria, the sample was reprocessed several times, each reprocessing entailing a variation of one of the selection criteria:

- track polar angle,
- track momentum,
- track impact parameter in z,
- track impact parameter in $R\phi$,
- sphericity axis polar angle.

For each of the reprocessings, the fragmentation function components were calculated by the weighting method, as described in Section 3. The difference of the components extracted for a given reprocessing from the components of the basic sample is the systematic error related to the criterion that was varied in this reprocessing. A detailed list of the systematic errors is given in [7].

The fragmentation function components can be extracted not only by the weighting method (5), but also by a direct fit to the angular distributions, with $F_T(x_p)$ and $F_L(x_p)$ being free parameters. The fit, as well as the weighting, can be performed in different angular intervals. Although mathematically both methods should give the same result, experimentally it is not the case, since the central points of the $\cos\theta$ distribution (around $\cos\theta = 0$) deviate strongly from the expected values, due to the configuration of the detector[1]. Therefore, systematic errors introduced by the method of extraction of the components of the fragmentation function were calculated from

- the difference between fit and weight results,
- variations of the range of the $\cos\theta$ values used in the extraction and
- the removal of central points in the $\cos\theta$ distributions.

For the first error, the differences were taken between F_T and F_L from weights and F_T and F_L from fits. For the second error, calculations by weights were used. Each calculation corresponded to a different value of v, with $v = 0.85$ being the value of the reference sample. The average value of the differences of F_T and F_L obtained from the reference sample and those obtained from the three others (absolute values) was considered

[1]The DELPHI TPC tension plate effectively produces a "shade" around $\cos\theta = 0$

as the systematic error due to the variation of v. The removal of central points in the $\cos\theta$ distributions was performed artificially as follows. The $\cos\theta$ distributions were first fitted with the four central points excluded from the fit. Then the values of the data in the four central bins were replaced by the corresponding values of the fitted function. The weighting method was subsequently applied to the modified $\cos\theta$ distributions to extract new values for F_T and F_L. These new values were subtracted from the values of the reference sample giving the errors for the exclusion of the central points in the $\cos\theta$ distributions.

All the contributions to the systematic uncertainty were added quadratically, and the result was given as the total systematic error. The errors are shown, e.g., in Tables 1 and 2.

4 Hadronization corrections

The analysis, described above, relies on the assumption that the angular distribution of hadrons corresponds to that one of original partons. However, due to the hadronization process specifics, hadrons are not emitted exactly along the direction of their parent parton, especially those carrying low x_p. This induces a distortion to the fragmentation function components. To lowest order, the contribution from the hadronization will be positive for F_L and negative for F_T, as can be deduced from the picture of a quark-antiquark pair moving back-to-back and producing a number of hadrons. The parton direction corresponds to the $1 + \cos^2\theta$ distribution in Eq.(1), therefore, if the hadrons were emitted along the direction of the initial partons, F_L would be vanishing. The smearing in the hadron p_T introduces a shift to a more isotropic picture, i.e. generates a $\sin^2\theta$ term in the angular distribution of the hadrons. This term is responsible for the appearance of a (positive) F_L component. F_T will be at the same time reduced, so that the sum of two remains constant. This non-vanishing component of F_L was extracted by running JETSET 7.4 with the parton shower switched off, i.e. while considering only $q\overline{q}$ events, and was found to be significant and mostly so at low x_p values. This was expected as the harder the hadron the closer it is emitted to the parent parton direction.

To correct the fragmentation function components for the fragmentation effect, the measurement should be performed not on the individual hadrons, but rather on clusters of them. The method is described in details in [8], and is outlined below.

4.1 Correction by clustering

One expects to have a larger angular smearing at low x_p values than at high ones. However, having the string fragmentation picture in mind, the string can also pull particles from a gluon jet towards a quark one (the string/drag effect [9, 10]). This means that the anisotropy introduced by the presence of the gluon will be reduced, i.e. the string is now giving a correction to F_T and F_L which has the opposite sign to the contribution from the fragmentation p_T smearing. To account for these effects, the clustering method was introduced in the analysis.

The DELPHI-tuned generator was used to generate 5 million events with no topology restrictions. Then, the Durham algorithm [11] was applied to cluster the stable hadrons (only charged particles were considered), with each cluster assumed to represent a mother parton. The direction of each cluster was thus thought of as the direction of a parton, each having a number of daughter hadrons associated to it. The correction entailed replacing the polar angle of hadrons by the polar angle of the associated cluster. The x_p of each hadron was not changed, and taken as it is. This resulted in having effectively events, where all hadrons were aligned with their parent partons, i.e. as in Eq.(1) assumed to be the case. Consequently, applying Eq.(1) to the cluster-deduced polar angle ($\cos\theta$) distributions of the charged hadrons would give fragmentation function components which are not affected by smearing effects during the fragmentation procedure.

The most important issue in such a method is to find a proper clustering cut-off scale. This issue was addressed in [8], where both charged and neutral particles in JETSET generated events were taken into account, and the clustering cut-off used was the scaled cut-off parameter of the Durham algorithm. However, only charged particles are considered in the real data. Therefore, instead of the scaled cut-off, the absolute Durham distance measure will be used in the following:

$$y_{ij} = \sqrt{2\,min(E_i^2, E_j^2)(1 - \cos\theta_{ij})}\ , \tag{7}$$

where E_i and E_j are the energies of clusters i and j , and $\cos\theta_{ij}$ is the angle between the momentum vectors of the two clusters. The distance measure, or cut-off parameter, y_{cut}, is the maximum distance, below which two clusters can be joined in one and corresponds roughly to the relative transverse momentum of the two clusters. From [8], the following values were considered for the cut-off parameter of the clustering: $y_{cut} = 0.912\ GeV$, $y_{cut} = 1.290\ GeV$ and $y_{cut} = 2.040\ GeV$. The correction procedure, using the JETSET event generator, is explained below.

For each value of y_{cut}, the output of the generator was two sets of $\cos\theta$ distributions, each distribution referring to an x_p bin as in the data (see Section 2). The first set of distributions was built using the actual polar angle θ of the charged hadrons. The second set used the polar angle of the clusters. The fragmentation function components F_T and F_L were then extracted for both hadrons and clusters.

From the Monte Carlo distributions thus obtained, a correction to the data can be calculated as the difference of the distributions of hadrons and clusters. The different normalization in data and Monte Carlo was taken into account, leading to a correction of the form:

$$F_P^{corrected} = F_P^{data} - \frac{(F_T + F_L)^{data}}{(F_T + F_L)^{MC}}(F_P^{hadrons} - F_P^{clusters})^{MC}\ , \tag{8}$$

where subscript P stands for either T or L, F_P^{data} is the original function as was extracted from the data and $F_P^{corrected}$ is the corrected one. The corrected fragmentation function components are given in Figures 2 and 3. The correlation between errors has been taken into account. As expected, the correction by clustering is significant for both helicity components, and especially so at low x_p values.

The fragmentation function components before and after the correction by clustering are given in Tables 1 and 2. The first error quoted is the statistical error and the second is the systematic one.

As was discussed in [8], there is no ideal value for the clustering cut-off, as it is not precisely known at which scale the hadronization process starts. Therefore, there is no unique answer for the helicity components of the fragmentation function, rather, a scale-dependent answer has to be considered.

Table 1: F_T from original data and corrected for the three values of the clustering cut-off (simulation correction).

x_p	F_T uncorrected	$F_T(y_{cut} = 0.912GeV)$	$F_T(y_{cut} = 1.290GeV)$	$F_T(y_{cut} = 2.040GeV)$
$0.00 \div 0.01$	$279.8 \pm 0.4 \pm 7.2$	$325.8 \pm 0.6 \pm 7.4$	$333.5 \pm 0.6 \pm 7.5$	$342.4 \pm 0.6 \pm 7.6$
$0.01 \div 0.02$	$323.8 \pm 0.4 \pm 4.1$	$345.5 \pm 0.5 \pm 4.1$	$351.9 \pm 0.5 \pm 4.1$	$360.2 \pm 0.5 \pm 4.2$
$0.02 \div 0.03$	$226.15 \pm 0.30 \pm 4.27$	$230.7 \pm 0.4 \pm 4.3$	$233.7 \pm 0.4 \pm 4.3$	$237.3 \pm 0.4 \pm 4.3$
$0.03 \div 0.04$	$165.51 \pm 0.25 \pm 3.35$	$166.8 \pm 0.4 \pm 3.4$	$167.8 \pm 0.4 \pm 3.4$	$169.8 \pm 0.4 \pm 3.4$
$0.04 \div 0.05$	$125.39 \pm 0.21 \pm 1.69$	$125.8 \pm 0.3 \pm 1.7$	$126.2 \pm 0.3 \pm 1.7$	$127.1 \pm 0.3 \pm 1.7$
$0.05 \div 0.06$	$98.07 \pm 0.19 \pm 2.36$	$98.24 \pm 0.26 \pm 2.37$	$98.53 \pm 0.26 \pm 2.37$	$98.95 \pm 0.26 \pm 2.37$
$0.06 \div 0.07$	$78.91 \pm 0.17 \pm 1.06$	$79.02 \pm 0.24 \pm 1.07$	$79.15 \pm 0.24 \pm 1.07$	$79.43 \pm 0.24 \pm 1.07$
$0.07 \div 0.08$	$64.65 \pm 0.15 \pm 0.86$	$64.69 \pm 0.21 \pm 0.87$	$64.73 \pm 0.21 \pm 0.87$	$64.92 \pm 0.21 \pm 0.87$
$0.08 \div 0.09$	$53.80 \pm 0.14 \pm 0.77$	$53.74 \pm 0.19 \pm 0.78$	$53.87 \pm 0.19 \pm 0.78$	$53.99 \pm 0.19 \pm 0.78$
$0.09 \div 0.10$	$45.48 \pm 0.13 \pm 1.12$	$45.47 \pm 0.18 \pm 1.12$	$45.45 \pm 0.18 \pm 1.12$	$45.54 \pm 0.18 \pm 1.12$
$0.10 \div 0.12$	$35.74 \pm 0.08 \pm 0.59$	$35.72 \pm 0.11 \pm 0.59$	$35.74 \pm 0.11 \pm 0.59$	$35.83 \pm 0.11 \pm 0.59$
$0.12 \div 0.14$	$26.86 \pm 0.07 \pm 0.37$	$26.85 \pm 0.10 \pm 0.38$	$26.87 \pm 0.10 \pm 0.38$	$26.90 \pm 0.10 \pm 0.38$
$0.14 \div 0.16$	$20.54 \pm 0.06 \pm 0.55$	$20.55 \pm 0.08 \pm 0.56$	$20.57 \pm 0.08 \pm 0.56$	$20.60 \pm 0.08 \pm 0.56$
$0.16 \div 0.18$	$16.10 \pm 0.05 \pm 0.35$	$16.12 \pm 0.08 \pm 0.36$	$16.12 \pm 0.08 \pm 0.36$	$16.13 \pm 0.08 \pm 0.36$
$0.18 \div 0.20$	$12.73 \pm 0.05 \pm 0.27$	$12.73 \pm 0.07 \pm 0.27$	$12.74 \pm 0.07 \pm 0.27$	$12.76 \pm 0.07 \pm 0.27$
$0.20 \div 0.25$	$8.727 \pm 0.025 \pm 0.340$	$8.72 \pm 0.03 \pm 0.34$	$8.73 \pm 0.03 \pm 0.34$	$8.74 \pm 0.03 \pm 0.34$
$0.25 \div 0.30$	$5.323 \pm 0.019 \pm 0.143$	$5.321 \pm 0.027 \pm 0.144$	$5.321 \pm 0.027 \pm 0.144$	$5.323 \pm 0.027 \pm 0.144$
$0.30 \div 0.40$	$2.710 \pm 0.010 \pm 0.113$	$2.709 \pm 0.014 \pm 0.114$	$2.709 \pm 0.014 \pm 0.114$	$2.709 \pm 0.014 \pm 0.114$
$0.40 \div 0.50$	$1.147 \pm 0.007 \pm 0.019$	$1.147 \pm 0.009 \pm 0.020$	$1.147 \pm 0.009 \pm 0.020$	$1.149 \pm 0.009 \pm 0.020$
$0.50 \div 0.60$	$0.503 \pm 0.004 \pm 0.034$	$0.504 \pm 0.006 \pm 0.034$	$0.503 \pm 0.006 \pm 0.034$	$0.502 \pm 0.006 \pm 0.034$
$0.60 \div 0.80$	$0.1598 \pm 0.0018 \pm 0.0320$	$0.1597 \pm 0.0023 \pm 0.0320$	$0.1598 \pm 0.0023 \pm 0.0320$	$0.1599 \pm 0.0023 \pm 0.0320$
$0.80 \div 1.00$	$0.0227 \pm 0.0007 \pm 0.0098$	$0.0227 \pm 0.0008 \pm 0.0098$	$0.0227 \pm 0.0008 \pm 0.0098$	$0.0227 \pm 0.0008 \pm 0.0098$

x_p	F_L uncorrected	$F_L(y_{cut} = 0.912 GeV)$	$F_L(y_{cut} = 1.290 GeV)$	$F_L(y_{cut} = 2.040 GeV)$
$0.00 \div 0.01$	$104.5 \pm 0.3 \pm 11.4$	$58.3 \pm 0.4 \pm 11.5$	$50.6 \pm 0.4 \pm 11.6$	$41.7 \pm 0.4 \pm 11.6$
$0.01 \div 0.02$	$79.37 \pm 0.28 \pm 5.00$	$57.7 \pm 0.4 \pm 5.0$	$51.2 \pm 0.4 \pm 5.0$	$42.9 \pm 0.4 \pm 5.0$
$0.02 \div 0.03$	$36.80 \pm 0.22 \pm 3.13$	$32.2 \pm 0.3 \pm 3.1$	$29.2 \pm 0.3 \pm 3.1$	$25.5 \pm 0.3 \pm 3.1$
$0.03 \div 0.04$	$18.66 \pm 0.19 \pm 3.27$	$17.40 \pm 0.26 \pm 3.28$	$16.32 \pm 0.26 \pm 3.28$	$14.41 \pm 0.26 \pm 3.28$
$0.04 \div 0.05$	$11.07 \pm 0.16 \pm 1.78$	$10.68 \pm 0.23 \pm 1.79$	$10.23 \pm 0.23 \pm 1.79$	$9.37 \pm 0.23 \pm 1.79$
$0.05 \div 0.06$	$6.91 \pm 0.14 \pm 2.27$	$6.77 \pm 0.20 \pm 2.28$	$6.49 \pm 0.20 \pm 2.28$	$6.06 \pm 0.20 \pm 2.28$
$0.06 \div 0.07$	$4.69 \pm 0.13 \pm 1.06$	$4.61 \pm 0.18 \pm 1.07$	$4.47 \pm 0.18 \pm 1.07$	$4.18 \pm 0.18 \pm 1.07$
$0.07 \div 0.08$	$3.26 \pm 0.11 \pm 0.82$	$3.25 \pm 0.16 \pm 0.83$	$3.19 \pm 0.16 \pm 0.83$	$3.00 \pm 0.16 \pm 0.83$
$0.08 \div 0.09$	$2.44 \pm 0.10 \pm 0.69$	$2.49 \pm 0.15 \pm 0.70$	$2.39 \pm 0.15 \pm 0.70$	$2.26 \pm 0.15 \pm 0.70$
$0.09 \div 0.10$	$1.71 \pm 0.10 \pm 0.62$	$1.72 \pm 0.13 \pm 0.63$	$1.72 \pm 0.13 \pm 0.63$	$1.64 \pm 0.13 \pm 0.63$
$0.10 \div 0.12$	$1.30 \pm 0.06 \pm 0.50$	$1.31 \pm 0.08 \pm 0.50$	$1.29 \pm 0.08 \pm 0.50$	$1.21 \pm 0.08 \pm 0.50$
$0.12 \div 0.14$	$0.67 \pm 0.05 \pm 0.36$	$0.69 \pm 0.07 \pm 0.36$	$0.67 \pm 0.07 \pm 0.36$	$0.63 \pm 0.07 \pm 0.36$
$0.14 \div 0.16$	$0.47 \pm 0.05 \pm 0.23$	$0.47 \pm 0.06 \pm 0.24$	$0.45 \pm 0.06 \pm 0.24$	$0.43 \pm 0.06 \pm 0.24$
$0.16 \div 0.18$	$0.25 \pm 0.04 \pm 0.33$	$0.24 \pm 0.06 \pm 0.33$	$0.23 \pm 0.06 \pm 0.33$	$0.23 \pm 0.06 \pm 0.33$
$0.18 \div 0.20$	$0.19 \pm 0.04 \pm 0.13$	$0.19 \pm 0.05 \pm 0.13$	$0.18 \pm 0.05 \pm 0.13$	$0.17 \pm 0.05 \pm 0.13$
$0.20 \div 0.25$	$0.116 \pm 0.018 \pm 0.170$	$0.119 \pm 0.026 \pm 0.171$	$0.117 \pm 0.026 \pm 0.171$	$0.106 \pm 0.026 \pm 0.171$
$0.25 \div 0.30$	$0.010 \pm 0.014 \pm 0.036$	$0.012 \pm 0.020 \pm 0.038$	$0.012 \pm 0.020 \pm 0.038$	$0.009 \pm 0.020 \pm 0.038$
$0.30 \div 0.40$	$0.021 \pm 0.007 \pm 0.045$	$0.022 \pm 0.010 \pm 0.045$	$0.022 \pm 0.010 \pm 0.045$	$0.021 \pm 0.010 \pm 0.045$
$0.40 \div 0.50$	$0.004 \pm 0.005 \pm 0.028$	$0.004 \pm 0.007 \pm 0.028$	$0.004 \pm 0.007 \pm 0.028$	$0.002 \pm 0.007 \pm 0.028$
$0.50 \div 0.60$	$0.000 \pm 0.003 \pm 0.022$	$-0.000 \pm 0.004 \pm 0.022$	$0.000 \pm 0.004 \pm 0.022$	$0.000 \pm 0.004 \pm 0.022$
$0.60 \div 0.80$	$-0.006 \pm 0.0013 \pm 0.0223$	$-0.006 \pm 0.0017 \pm 0.0223$	$-0.006 \pm 0.0017 \pm 0.0223$	$-0.0062 \pm 0.0017 \pm 0.0223$
$0.80 \div 1.00$	$-0.0035 \pm 0.0005 \pm 0.0070$	$-0.0035 \pm 0.0006 \pm 0.0070$	$-0.0035 \pm 0.0006 \pm 0.0070$	$-0.0035 \pm 0.0006 \pm 0.0070$

Table 2: F_L from original data and corrected for the three values of the clustering cut-off (simulation correction).

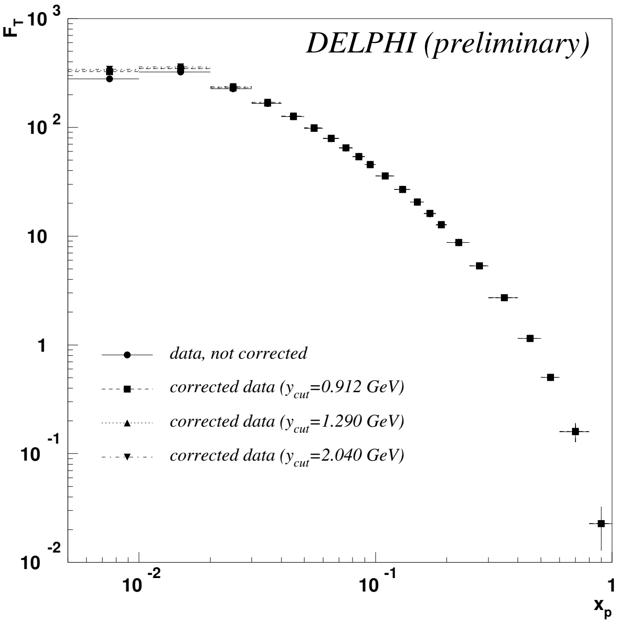

Figure 2: F_T from original data and F_T corrected for the fragmentation effect by clustering. The corrected component is given for three values of the cut-off parameter, y_{cut}, of the Durham clustering algorithm.

As the results presented in this section involve a rather substantial correction which relies on the JETSET generator, an effort was made to extract the same information, *i.e.*, the corrected functions, directly from data. This is described in the following section.

4.2 Clustering data

To avoid a model-dependent correction in the measurement of the fragmentation function components, the data were reprocessed to apply the clustering directly on the measured particles. The clustering was performed by the same algorithm and for the same values of the cut-off parameter as discussed in Section 4.1. For each clustering parameter, the helicity components of the fragmentation function were extracted from the distributions of $\cos\theta$ of clusters and x_p of hadrons.

The fragmentation function components for the three clustering cut-offs are shown in Figures 4 and 5, and in Tables 3 and 4. The agreement with the Monte Carlo corrected functions is seen to be good. This gives confidence to the measurement of the helicity components presented in this report, so that the can be used to extract information about the strong coupling constant, α_s (see Section 5).

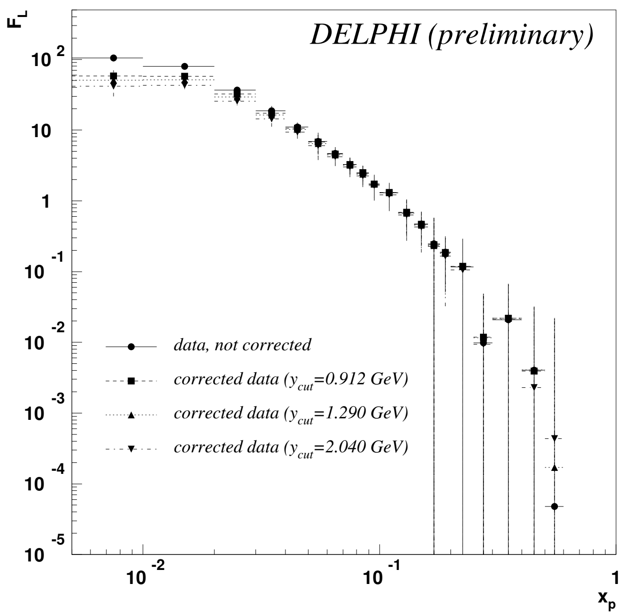

Figure 3: F_L from original data and F_L corrected for the fragmentation effect by clustering. The corrected component is given for three values of the cut-off parameter, y_{cut}, of the Durham clustering algorithm.

x_p	$F_T(y_{cut} = 0.912GeV)$	$F_T(y_{cut} = 1.290GeV)$	$F_T(y_{cut} = 2.040GeV)$
$0.00 \div 0.01$	$326.2 \pm 0.5 \pm 7.1$	$335.3 \pm 0.5 \pm 8.9$	$345.9 \pm 0.5 \pm 11.2$
$0.01 \div 0.02$	$340.5 \pm 0.4 \pm 9.3$	$346.7 \pm 0.4 \pm 9.7$	$355.0 \pm 0.5 \pm 10.4$
$0.02 \div 0.03$	$231.3 \pm 0.3 \pm 4.1$	$233.7 \pm 0.3 \pm 4.7$	$237.0 \pm 0.3 \pm 5.1$
$0.03 \div 0.04$	$167.41 \pm 0.26 \pm 2.59$	$168.36 \pm 0.28 \pm 2.73$	$169.75 \pm 0.28 \pm 3.04$
$0.04 \div 0.05$	$126.15 \pm 0.23 \pm 2.11$	$126.60 \pm 0.23 \pm 2.46$	$127.30 \pm 0.24 \pm 3.22$
$0.05 \div 0.06$	$98.45 \pm 0.20 \pm 2.21$	$98.79 \pm 0.20 \pm 2.17$	$99.11 \pm 0.20 \pm 2.14$
$0.06 \div 0.07$	$79.06 \pm 0.18 \pm 1.27$	$79.26 \pm 0.18 \pm 1.74$	$79.50 \pm 0.18 \pm 1.83$
$0.07 \div 0.08$	$64.78 \pm 0.16 \pm 1.23$	$64.81 \pm 0.16 \pm 1.03$	$64.97 \pm 0.16 \pm 1.30$
$0.08 \div 0.09$	$53.94 \pm 0.15 \pm 0.75$	$54.03 \pm 0.15 \pm 0.78$	$54.18 \pm 0.15 \pm 0.87$
$0.09 \div 0.10$	$45.57 \pm 0.13 \pm 1.00$	$45.57 \pm 0.14 \pm 1.01$	$45.61 \pm 0.14 \pm 0.80$
$0.10 \div 0.12$	$35.77 \pm 0.08 \pm 0.45$	$35.83 \pm 0.08 \pm 0.44$	$35.89 \pm 0.08 \pm 0.46$
$0.12 \div 0.14$	$26.89 \pm 0.07 \pm 0.27$	$26.92 \pm 0.07 \pm 0.29$	$26.97 \pm 0.07 \pm 0.24$
$0.14 \div 0.16$	$20.49 \pm 0.06 \pm 0.69$	$20.51 \pm 0.06 \pm 0.48$	$20.53 \pm 0.06 \pm 0.36$
$0.16 \div 0.18$	$16.09 \pm 0.06 \pm 0.37$	$16.10 \pm 0.06 \pm 0.39$	$16.13 \pm 0.06 \pm 0.22$
$0.18 \div 0.20$	$12.71 \pm 0.05 \pm 0.17$	$12.72 \pm 0.05 \pm 0.17$	$12.73 \pm 0.05 \pm 0.26$
$0.20 \div 0.25$	$8.716 \pm 0.025 \pm 0.279$	$8.715 \pm 0.026 \pm 0.255$	$8.722 \pm 0.026 \pm 0.292$
$0.25 \div 0.30$	$5.311 \pm 0.019 \pm 0.127$	$5.319 \pm 0.020 \pm 0.115$	$5.328 \pm 0.020 \pm 0.181$
$0.30 \div 0.40$	$2.709 \pm 0.009 \pm 0.070$	$2.713 \pm 0.010 \pm 0.050$	$2.717 \pm 0.010 \pm 0.061$
$0.40 \div 0.50$	$1.142 \pm 0.007 \pm 0.049$	$1.142 \pm 0.007 \pm 0.039$	$1.142 \pm 0.007 \pm 0.041$
$0.50 \div 0.60$	$0.502 \pm 0.005 \pm 0.049$	$0.503 \pm 0.005 \pm 0.085$	$0.502 \pm 0.005 \pm 0.096$
$0.60 \div 0.80$	$0.1593 \pm 0.0018 \pm 0.0384$	$0.1591 \pm 0.0018 \pm 0.0366$	$0.1588 \pm 0.0018 \pm 0.0348$
$0.80 \div 1.00$	$0.0225 \pm 0.0007 \pm 0.0084$	$0.0226 \pm 0.0007 \pm 0.0088$	$0.0226 \pm 0.0007 \pm 0.0100$

Table 3: F_T from clustered data for the three values of Durham cut-off.

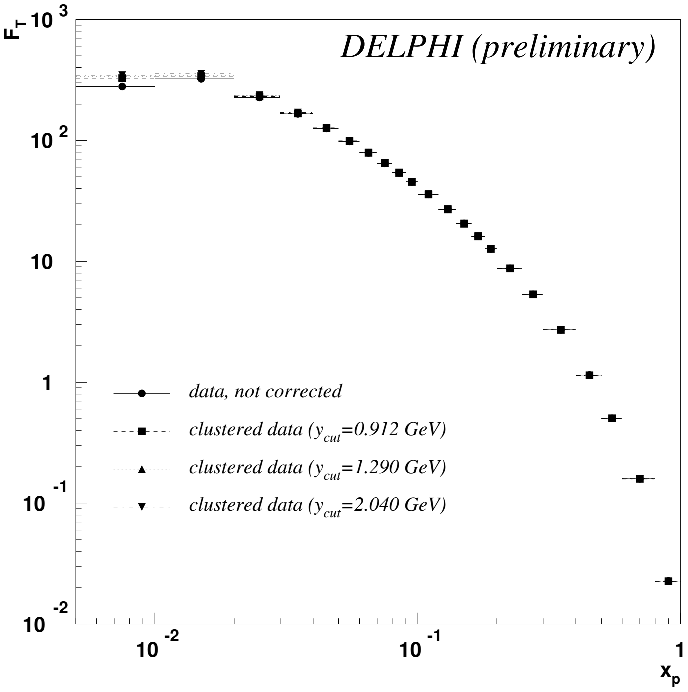

Figure 4: F_T from original data and F_T from clustered data. The clustered components are given for three values of the cut-off parameter, y_{cut}, for the Durham clustering algorithm.

5 The strong coupling constant

The strong coupling constant was extracted from the second moments (σ_L) of F_L distributions presented in the previous section, using the following NLO equation [12]

$$\frac{\sigma_L}{\sigma_{tot}} = \frac{\alpha_s}{\pi} + \frac{\alpha_s^2}{\pi^2}(13.583 - N_f \cdot 1.028) \ , \tag{9}$$

where N_f is the number of active flavours.

As this relation implies that both charged and neutral particles have been included in the definition of σ_L, a correction was required for having neglected the neutral ones. This correction was obtained by using the DELPHI-tuned JETSET generation to calculate the ratio of σ_L for all particles (referred to as σ_L^{all}) to σ_L for charged particles only (σ_L^{ch}). The calculation was done using uncorrected (for the hadronization effects), as well as those corrected using different y_{cut} values. The results are given in Table 5. It can be seen that the correction is nearly 100%, and slightly depends on the y_{cut} value.

The normalized longitudinal cross sections σ_L^{ch} from the data were then corrected by multiplication with the correction factor of Table 5. The cross sections before and after the correction for the neutral particles are given in Table 6. In the last column of the table, the corresponding values of the strong coupling constant α_s are given, as deduced using Eq.(9). The strong coupling constant values given in Table 6 are somewhat low in comparison with the values obtained from event shape studies or from the scaling violation analysis. The value of α_s is also seen to be slightly dependent on y_{cut}, however, all the results are within the error margins.

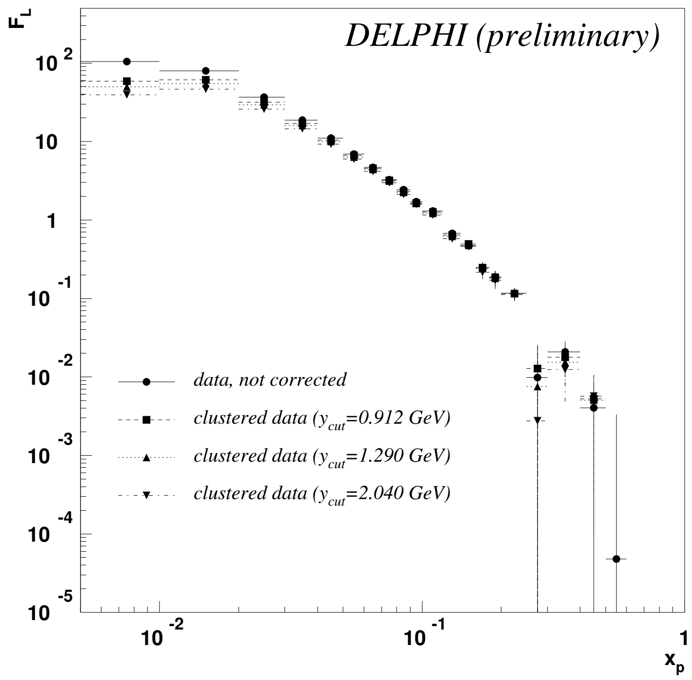

Figure 5: F_L from original data and F_L from clustered data. The clustered components are given for three values of the cut-off parameter, y_{cut}, for the Durham clustering algorithm.

To estimate whether there is a significant dependence of the calculation of σ_L on the clustering algorithm, simulated events where clustered using the JADE algorithm [13] instead of Durham. This was done for a sample of 5 million events generated with the DELPHI-tuned generator. The clustering cut-off for JADE was selected so as to give approximately the same mean cluster multiplicity as the middle Durham cut-off ($y_{cut}^{Durham} = 1.290\ GeV$). Corresponding y_{cut}^{JADE} was found to be 2.192 GeV, giving a mean number of clusters equal to 5.164 ± 0.001 (to be compared with 5.162 ± 0.001 clusters for Durham). The calculated σ_L^{ch} for Jade was 0.0303 ± 0.0024 (to be compared with 0.0292 ± 0.0019 for Durham). This shows that the analysis is not sensitive to the choice of the clustering algorithm.

As is discussed in [8], clustering at parton and hadron level showed the best agreement for a "clustering" scale around 1.3 GeV, and therefore the corresponding to that cut-off value of α_s might be considered as a preferred value. However, it should perhaps be stressed that this value depends on the model and should be treated carefully. Therefore, a more conservative approach would be to consider the spread of the values of obtained for the different clustering cut-off values as an uncertainty stemming from the hadronization correction procedure.

6 Summary

The fragmentation function analysis presented in this report concentrates on the extraction of the transverse and longitudinal components of the fragmentation function and

x_p	$F_L \pm (y_{cut} = 0.912 GeV)$	$F_L(y_{cut} = 1.290 GeV)$	$F_L(y_{cut} = 2.040 GeV)$
$0.00 \div 0.01$	$58.6 \pm 0.4 \pm 8.6$	$49.8 \pm 0.4 \pm 7.5$	$39.5 \pm 0.4 \pm 6.9$
$0.01 \div 0.02$	$61.3 \pm 0.3 \pm 9.3$	$55.0 \pm 0.3 \pm 9.4$	$46.5 \pm 0.3 \pm 9.5$
$0.02 \div 0.03$	$31.87 \pm 0.24 \pm 4.04$	$29.27 \pm 0.25 \pm 4.63$	$25.87 \pm 0.25 \pm 4.92$
$0.03 \div 0.04$	$16.96 \pm 0.20 \pm 2.65$	$16.00 \pm 0.21 \pm 2.51$	$14.51 \pm 0.21 \pm 2.61$
$0.04 \div 0.05$	$10.43 \pm 0.17 \pm 2.00$	$9.98 \pm 0.17 \pm 2.06$	$9.24 \pm 0.18 \pm 2.43$
$0.05 \div 0.06$	$6.62 \pm 0.15 \pm 2.12$	$6.31 \pm 0.15 \pm 2.04$	$5.97 \pm 0.15 \pm 1.99$
$0.06 \div 0.07$	$4.56 \pm 0.13 \pm 1.30$	$4.40 \pm 0.13 \pm 1.60$	$4.16 \pm 0.14 \pm 1.66$
$0.07 \div 0.08$	$3.18 \pm 0.12 \pm 1.01$	$3.14 \pm 0.12 \pm 0.97$	$2.98 \pm 0.12 \pm 1.09$
$0.08 \div 0.09$	$2.33 \pm 0.11 \pm 0.84$	$2.25 \pm 0.11 \pm 0.92$	$2.12 \pm 0.11 \pm 0.91$
$0.09 \div 0.10$	$1.64 \pm 0.10 \pm 0.81$	$1.63 \pm 0.10 \pm 0.75$	$1.58 \pm 0.10 \pm 0.68$
$0.10 \div 0.12$	$1.27 \pm 0.06 \pm 0.59$	$1.21 \pm 0.06 \pm 0.66$	$1.16 \pm 0.06 \pm 0.63$
$0.12 \div 0.14$	$0.64 \pm 0.05 \pm 0.39$	$0.62 \pm 0.05 \pm 0.44$	$0.58 \pm 0.05 \pm 0.34$
$0.14 \div 0.16$	$0.50 \pm 0.05 \pm 0.33$	$0.48 \pm 0.05 \pm 0.24$	$0.46 \pm 0.05 \pm 0.26$
$0.16 \div 0.18$	$0.25 \pm 0.04 \pm 0.38$	$0.24 \pm 0.04 \pm 0.40$	$0.22 \pm 0.04 \pm 0.31$
$0.18 \div 0.20$	$0.19 \pm 0.04 \pm 0.12$	$0.18 \pm 0.04 \pm 0.16$	$0.17 \pm 0.04 \pm 0.13$
$0.20 \div 0.25$	$0.116 \pm 0.019 \pm 0.133$	$0.116 \pm 0.019 \pm 0.135$	$0.112 \pm 0.019 \pm 0.177$
$0.25 \div 0.30$	$0.013 \pm 0.015 \pm 0.057$	$0.008 \pm 0.015 \pm 0.056$	$0.003 \pm 0.015 \pm 0.063$
$0.30 \div 0.40$	$0.018 \pm 0.007 \pm 0.022$	$0.015 \pm 0.007 \pm 0.036$	$0.012 \pm 0.008 \pm 0.042$
$0.40 \div 0.50$	$0.005 \pm 0.005 \pm 0.048$	$0.005 \pm 0.005 \pm 0.042$	$0.006 \pm 0.005 \pm 0.026$
$0.50 \div 0.60$	$-0.000 \pm 0.003 \pm 0.032$	$-0.001 \pm 0.003 \pm 0.056$	$-0.000 \pm 0.003 \pm 0.063$
$0.60 \div 0.80$	$-0.0061 \pm 0.0013 \pm 0.0265$	$-0.0060 \pm 0.0013 \pm 0.0254$	$-0.0057 \pm 0.0013 \pm 0.0241$
$0.80 \div 1.00$	$-0.0035 \pm 0.0005 \pm 0.0059$	$-0.0034 \pm 0.0005 \pm 0.0060$	$-0.0034 \pm 0.0005 \pm 0.0069$

Table 4: F_L from clustered data for the three values of Durham cut-off.

y_{cut}	σ_L	σ_L^{ch}	$\sigma_L^{ch}/\sigma_L^{all}$
—	0.0600 ± 0.0002	0.0339 ± 0.0002	0.5650 ± 0.0033
$0.912 GeV$	0.0549 ± 0.0002	0.0307 ± 0.0002	0.5592 ± 0.0036
$1.290 GeV$	0.0528 ± 0.0002	0.0292 ± 0.0002	0.5530 ± 0.0038
$2.040 GeV$	0.0492 ± 0.0002	0.0268 ± 0.0002	0.5447 ± 0.0041

Table 5: Correction factor for neglecting the neutral particles in the analysis. The cross sections have been calculated using the tuned simulation.

y_{cut}	σ_L^{ch}	σ_L	α_s
—	$0.0300 \pm 0.0003 \pm 0.0027$	$0.0531 \pm 0.0006 \pm 0.0048$	$0.1249 \pm 0.0011 \pm 0.0090$
$0.912 GeV$	$0.0263 \pm 0.0003 \pm 0.0031$	$0.0470 \pm 0.0006 \pm 0.0056$	$0.1132 \pm 0.0012 \pm 0.0109$
$1.290 GeV$	$0.0246 \pm 0.0003 \pm 0.0033$	$0.0445 \pm 0.0006 \pm 0.0060$	$0.1083 \pm 0.0012 \pm 0.0119$
$2.040 GeV$	$0.0223 \pm 0.0003 \pm 0.0034$	$0.0409 \pm 0.0006 \pm 0.0062$	$0.1010 \pm 0.0012 \pm 0.0126$

Table 6: Longitudinal cross sections from data and the strong coupling constant.

the hadronization correction required. The analysis has shown that the hadronization correction is mostly important for the longitudinal component and at low momentum values. The following method for the hadronization correction of the fragmentation function components has been considered. A clustering of the particles was introduced in order to bring the event backwards in time, namely approximately at the moment where the non-perturbative regime begins. This strategy has been applied both in terms of a Monte Carlo correction and directly to the data. The two results showed nice agreement. The clustering method therefore seems to be a good approach for accounting for hadronization. However, it introduces an uncertainty in the cut-off scale itself. A reasonable range of scales has therefore been selected. The corrected longitudinal component of the fragmentation function was used to extract the strong coupling constant, α_s. As the fragmentation functions depend on the cut-off scale of the clustering, this implies an uncertainty for the value of. The preferred value for y_{cut} gives

$$\alpha_s = 0.1083 \pm 0.0012 \pm 0.0119$$

References

[1] DELPHI Coll., P.Abreu et al., Eur. Phys. J. **C6** (1999) 19.

[2] OPAL Coll., R. Akers et al., Z. Phys. **C68** (1995) 203.

[3] ALEPH Coll., D. Buskulic et al., Phys. Lett. **B357** (1995) 487.

[4] P. Nason and B. R. Webber, Nucl. Phys. **B421** (1994) 473, *e*rratum **B480** (1996) 755.

[5] DELPHI Coll., P. Abreu et al., Z. Phys. **C73** (1996) 11.

[6] T. Sjöstrand, Comp. Phys. Communications 39 (1986) 347; T. Sjöstrand and M. Bengtsson, Comp. Phys. Communications 43 (1987) 367; T. Sjöstrand, Comp. Phys. Communications 82 (1994) 74.

[7] Ch. Zacharatou Jarlskog, Luminosity evaluation and fragmentation studies for the DELPHI experiment at LEP, LUNFD6/(NFFL-7193) 2001, PhD thesis.

[8] T. Sjöstrand, O. Smirnova and Ch. Zacharatou Jarlskog, hep-ph/0104118, to be published in Eur. Phys. J. C.

[9] B. Andersson, G. Gustafson and T. Sjöstrand, Phys. Lett. **94B** (1980) 211.

[10] Ya. I. Azimov, Yu. L. Dokshitzer, V. A. Khoze and S. I. Troyan, Phys. Lett. **165B** (1985) 147.

[11] S. Catani, Yu. L. Dokshitzer, M. Olsson, G. Turnock and B. R. Webber, Phys. Lett. **B269** (1991) 432.

[12] P. J. Rijken, W. L. van Neerven, Phys. Lett. **B386** (1996) 422.

[13] JADE Coll., W. Bartel et al., Z. Phys. **C33** (1986) 23.